05,10

Nonlinear dynamics of a semi-infinite ferromagnet with the helicoidal structure

© V.V. Kiselev[1,2], A.A. Raskovalov[1,2,3,¶]

[1] M.N. Mikheev Institute of Metal Physics, Ural Branch, Russian Academy of Sciences, Yekaterinburg, Russia
[2] Ural Federal University after the first President of Russia B.N. Yeltsin, Institute of Physics and Technology (UrFU), Yekaterinburg, Russia
[3] Skolkovo Institute of Science and Technology, Moscow, Russia

¶ E-mail: raskovalov@imp.uran.ru

Received April 5, 2024
Revised September 6, 2024
Accepted September 16, 2024

For easy-plane ferromagnet without inversion center new types of solitons, built into the helicoidal structure of the semi-infinite sample, are found and analyzed, based on the Landau–Lifshitz model. The mixed boundary conditions are used. Their limiting cases correspond to free or completely pinned spins at the boundary of the sample. All chiral solitons are travelling. It is shown, that their cores near the surface of the sample are dramatically deformed. This process is accompanied by remagnetization of the medium. The dynamical properties of the chiral solitons and peculiarities of their elastic reflection from the edge of the sample are analyzed, depending on the character of pinning of the edge spins.

Keywords: solitons, Landau–Lifshitz equation, turning wave, easy-plane anisotropy, chiral breather.

DOI: 10.61011/PSS.2024.10.59628.150

1. Introduction

During last decade extensive attention is drawn to magnetic materials, which main state is helical structure In crystals without the inversion center the helical ordering is frequently associated with Dzyaloshinski–Morii interaction, which is theoretically described by Lifshitz invariants in free energy decomposition [1–4]. Dzyaloshinski–Morii interaction compete with exchange interaction turning spins relatively to each other by small angle. Many papers (see for example [5–11]) relate to study of the physical properties of materials with helicoidal structure. Detail summary of theory of uniaxial ferromagnetics with helicoidal main state is provided in paper [12].

When switching on eternal magnetic field perpendicular to axis of the helicoidal structure the magnetic spiral with constant pitch is converted into one-dimensional lattice of extended domains. Inside each of them the magnetization distribution is close to homogeneous. The neighboring domains are separated by narrow domain walls — topological solitons, where helical turn of magnetization is localized. The solitons comprising the lattice due to their mobility and magnetoresistive properties are promising for use in spintronics devices. Study of movement and stability of some domain walls and lattice in general under the action of electric field is of great interest [13–16].

The helical ordering is implemented in rare-earth metals, in large class of conductive cubic magnetics without inversion center and in some other compounds. Among the known uniaxial helimagnetics ($CrNb_3S_6$, $CrTaS_6$, CuB_2O_4, $CuCsCl_3$, $Yb(Ni_{1-x}Cu_x)_3Al_9$, $Ba_2CuGe_2O_7$) [17–22] $CrNb_3S_6$ is more extensively studied. The lattice of chiral solitons was observed in experiments [23].

The chiral multisolitons build in helicoid structure of the ferromagnetics have useful technological properties [12,24]. But their analytical description is associated with many problems due to nonlinearity of the basic equations of the theory, and due to heterogeneity of helical ordering of the environment. Here we study the collective particle-like excitations of helicoidal structure, which in the magnetic field orthogonal to the axis of magnetic spiral is itself significantly nonlinear lattice of solitons. Hence, we have a little number of studies relating this theme. The problem can be solved with use of simplified models, which correctly consider the basic interactions, and at the same time allow accurate solutions. One of the models is a popular quasi-one-dimensional sine-Gordon equation. In infinite medium with homogeneous ground state it is completely integrated by the most effective method of nonlinear physics — by method of inverse scattering problem. Presence of the non-trivial ground state complicates the making of particle like excitations even in case of unlimited medium. The simple chiral solitons in the lattice of solitons were obtained by Backlund conversion in paper [25]. The complete study of the multisolitons and spin waves in the helicoidal structure based on the method of inverse scattering problem under

the sine–Gordon model can be found in monograph [26] (see also [27,28]).

Another effective model of chiral ferromagnetic is associated with quasi-one-dimensional Landau–Lifshitz equations if the magnetic field is absent. Recall that during analysis of low amplitude wave spectrum in Heisenberg ferromagnetic with Dzyaloshinski interaction and magnetic ordering with constant pitch the Landau−Lifshitz equation is frequently written in local benchmark, that shifts along the spiral axis (see, for example, [12] and papers cited in it). Then in new reference system the homogeneous ordering corresponds to homogeneous distribution of magnetization, and the spin wave dynamics is described by linearized Landau−Lifshitz equation for the ferromagnetic with exchange interaction without Dzyaloshinski interaction, but with additional anisotropy of „easy-plane" type. Papers [5,26,29] determined a deep relationship between accurate solutions of significantly nonlinear Landau−Lifshitz model for the ferromagnetic with the helicoidal structure considering the exchange energy, Dzyaloshinski interaction and energy of quadratic in magnetization uniaxial anisotropy (the anisotropy axis is parallel to Dzyaloshinski vector), and the solutions of equivalent model of uniaxial ferromagnetics without Dzyaloshinski interaction. The found relationship permits the use of soliton solutions of completely integrated equations of unlimited uniaxial ferromagnetic with homogeneous ground state to make and to analyze the spin waves and non-trivial multisolitons (moving or in rest) in the ferromagnetic with helicoidal structure. In general, the presence of magnetization easy axis coinciding with the direction of Dzyaloshinski vector suppresses the helicoidal ordering and keeps the metastable turn of magnetization in localized regions inside the sample only. For non-integrable one-dimensional Landau−Lifshitz equations this statement is justified by approximate methods in papers [15,16]. For integrated models of easy axis ferromagnetics the formation of nuclei of chiral phase on the background of homogeneous distribution of magnetization is analytically described in [5,29]. On the contrary, the quadratic in magnetization easy-plane anisotropy (base plane is parallel to plane of spin turn) keeps the helicoidal structure along full length of the sample. The particle-like solitons on the background of unlimited magnetic spiral are identified and analyzed in [5,29].

Actual samples have boundaries. Consideration of boundary conditions results in change of configuration of the helicoidal structure [12,30], and occurrence of important for applications features of dynamics of magnetic solitons and spin waves, which are absent in infinite medium. Besides, extension of the method of inverse spectral conversion to samples with finite size faces to serious problems due to absence of simple representation of initial boundary conditions for Landau−Lifshitz models in these scatterings. Such representation is possible under special (integrable) boundary conditions only [31,32].

For finite ferromagnetics without Dzyaloshinski interaction the physically meaningful integrable conditions were established quite a while [33]. But nonlinear dynamics of finite samples, also without helicoidal structure till now is not studied because there is no effective scheme of inverse spectral conversion for the finite systems. In papers [34,35] this problem was solved for the nonlinear Schrödinger equation by combination of the method of inverse scattering problem with „method of images", which is used in electrostatics when solving linear boundary problems with definite spatial symmetry. In papers [36–39] we used a scheme [34,35] to study solitons in the semi-infinite samples of Heisenberg ferromagnetic and uniaxial ferromagnetics with homogeneous ground state. Here we use these results for analytical description of the spin waves and solitons in the helicoidal structure of semi-infinite ferromagnetic.

We succeeded to summarize the conversion of papers [5,29] and to determine relationship between solutions of Landau−Lifshitz model for the semi-infinite uniaxial ferromagnetic without Dzyaloshinski interaction and the solutions of Landau−Lifshitz equations for the semi-infinite chiral ferromagnetic at boundary conditions considering the partial securing of spins at the boundary of sample. Using method of integration of Landau−Lifshitz equations of semi-infinite ferromagnetics with homogeneous ground state [37–39] the determined conversion provides full analytical description of the multisolitons and dispersive waves in semi-infinite chiral ferromagnetic with uniaxial magnetic anisotropy. Here we limit to discussion of the ferromagnetic with anisotropy of „easy-plane" type. Such type of the uniaxial anisotropy does not suppress the quasi-one-dimensional helicoidal structure in the sample bulk and results in non-trivial particle-like excitations on the background of magnetic spiral.

2. Semi-infinite ferromagnetic with homogeneous ground state

Let's provide basic formulas for the semi-infinite ferromagnetic with homogeneous ground state and homogeneous distribution of magnetization in sample depth [38,39], which are further used for the analytical description of solitons and waves in the helicoidal structure on half-axis $0 \le z < \infty$. Energy of such ferromagnetic with anisotropy of „easy-plane" type (plane Oxy) looks as follows [1]

$$E = \frac{1}{2}\int_0^\infty \mathrm{d}z \left[\alpha(\partial_z \mathbf{M})^2 + K(\mathbf{M}\cdot\mathbf{e}_3)^2\right] + H(\mathbf{M}\cdot\mathbf{e}_1)|_{z=0},$$

where $\mathbf{M}(z,t)$ — magnetization per unit of length along axis Oz ($\mathbf{M}^2 = M_0^2 = \mathrm{const}$), z and t — spatial coordinate and time, $\alpha > 0$ and $K > 0$ — constants of exchange interaction and anisotropy. Parameter H characterizes the effective field of unidirectional surface anisotropy $H = E_0/M_0$ determined by deposition of ferromagnetic layer on surface of ferromagnetic sample [40–42]. Here E_0 — exchange energy of unit of surface of sample. Its values for wide class of double-layer structures antiferromagnetic−ferromagnetic are

given in [43]. Single vectors $\mathbf{e}_1 = (1, 0, 0)$ and $\mathbf{e}_3 = (0, 0, 1)$ specify directions of the surface layer and „hard axis“ of magnetization, respectively.

In the dimensionless variables:

$$\mathbf{m} = -\mathbf{M}/M_0, \quad z' = z\sqrt{K/\alpha},$$

$$t' = \gamma M_0 K t, \quad h' = H M_0^{-1}/\sqrt{\alpha K}, \tag{1}$$

where γ — magnetomechanic ratio, system energy is

$$E' = \frac{E}{M_0^2\sqrt{\alpha K}} = \frac{1}{2}\int\limits_0^\infty \mathrm{d}z'[(\partial_{z'}\mathbf{m})^2 + m_3^2] - h' m_1|_{z=0}.$$

Possible nonlinear excitations in semi-infinite sample correspond to solutions of Landau–Lifshitz equation [26,44,45]:

$$\partial_{t'}\mathbf{m} = [\mathbf{m} \times \partial_{z'}^2\mathbf{m}] - (\mathbf{e}_3 \cdot \mathbf{m})[\mathbf{m} \times \mathbf{e}_3],$$

$$\mathbf{m}^2 = 1, \quad 0 \le z < \infty, \tag{2}$$

with integrated boundary conditions

$$[\mathbf{m} \times (\partial_{z'}\mathbf{m} + \mathbf{e}_1 h')]|_{z=0} = 0, \tag{3}$$

$$\mathbf{m} \to (1, 0, 0), \quad \partial_{z'}\mathbf{m} \to 0 \quad \text{at} \quad z' \to +\infty \tag{4}$$

and initial distribution of magnetization

$$\mathbf{m}(z', t' = 0) = \mathbf{m}_0(z'). \tag{5}$$

Selection of asymptotic boundary condition (4) corresponds to minimum of density of medium energy at $z' \gg 1$. Initial perturbation (5) is in agreement with conditions (3), (4). „Dashes“ above dimensionless variables are further omitted.

The mixed boundary condition (3) at $h \to 0$ transits into the condition of problem with free surface spins [45]:

$$[\mathbf{m} \times \partial_z \mathbf{m}]|_{z=0} = 0.$$

In limit $|h| \to \infty$ it comes down to the condition of full securing of spins at the sample boundary:

$$m_1|_{z=0} = \pm 1. \tag{6}$$

Sign selection in the right part (6) depends on type of solitons [38,39]. It will be clarified during further analysis.

The soliton evolution near the sample boundary can be formally explained as a result of interaction between the actual soliton inside the sample and the dummy soliton of image outside the sample. During interaction with the sample surface in the soliton localization region the magnetization shifts and turns occur by the value of about saturation magnetization. Scenarios of solitons reflection depend on the nature of securing of boundary spins. After reflection from the sample surface and by movement into the medium all solitons restore stationary shape, typical for solitons of the infinite medium.

Papers [38,39] showed that solitons of the semi-infinite easy-plane ferromagnetic are divided into two classes. The first class includes the solitons which cores upon movement away from the sample boundary undertake the shape of waves of stationary profile without internal oscillations of magnetization. Such solitons are not fixed. The magnetization distribution in the simplest of them looks like

$$m_1 = -1 + 2\,\mathrm{th}^2\rho(1 - n_1 n_2)^2 d^{-1},$$

$$m_2 = -2\,\mathrm{th}^2\rho(n_1 + n_2)(1 - n_1 n_2)d^{-1},$$

$$m_3 = 2\,\mathrm{sh}\,\rho(n_2 - n_1)(1 - n_1 n_2)/(d\,\mathrm{ch}^2\rho),$$

$$d = (n_1 - n_2)^2 + (1 + n_1 n_2)^2\,\mathrm{th}^2\rho,$$

$$n_1 = c_0 \exp\left(-\frac{z}{\mathrm{ch}\,\rho} + \frac{\mathrm{sh}\,\rho}{\mathrm{ch}^2\rho}\,t\right),$$

$$n_2 = \frac{f}{c_0}\exp\left(-\frac{z}{\mathrm{ch}\,\rho} - \frac{\mathrm{sh}\,\rho}{\mathrm{ch}^2\rho}\,t\right), \; f = \frac{h\,\mathrm{ch}\,\rho + 1}{h\,\mathrm{ch}\,\rho - 1}, \tag{7}$$

where c_0 — real constant of integration, $-\infty < \rho < \infty$ — solution parameter. Next, for certainty, we consider $\rho > 0$. As befits, the solution (7) meets the boundary conditions (3), (4).

In weak surface fields $|h| < \mathrm{ch}^{-1}\rho$ the parameter is $f < 0$, and, vice versa, $f > 0$ at $|h| > \mathrm{ch}^{-1}\rho$. This is observed in various scenarios of deformation of soliton core (7) during interaction with the sample boundary, and results in differences in its steady profile in sample depth before and after reflection from surface. In both cases all spins inside the soliton are inclined to the sample boundary at $c_0 > 0$ or into medium at $c_0 < 0$.

Let's explain the statement on the example of weak fields $|h| < \mathrm{ch}^{-1}\rho$. Them detail record of solution (7)

$$m_1 = -1 + \frac{2}{\tau}\,\mathrm{th}^2\rho\,\mathrm{ch}^2 y, \; y = \frac{z}{\mathrm{ch}\,\rho} - \frac{1}{2}\ln|f|,$$

$$m_2 = -\frac{2\,\mathrm{sign}\,c_0}{\tau}\,\mathrm{th}^2\rho\,\mathrm{sh}\,s\,\mathrm{ch}\,y,$$

$$s = \frac{\mathrm{sh}\,\rho}{\mathrm{ch}^2\rho}(t - t_0), \quad t_0 = \frac{\mathrm{ch}^2\rho}{2\,\mathrm{sh}\,\rho}\ln\frac{|f|}{c_0^2},$$

$$m_3 = -\frac{2\,\mathrm{sign}\,c_0}{\tau\,\mathrm{ch}^2\rho}\,\mathrm{sh}\,\rho\,\mathrm{ch}\,s\,\mathrm{ch}\,y, \; \tau = \mathrm{ch}^2 s + \mathrm{th}^2\rho\,\mathrm{sh}^2 y \tag{8}$$

exactly shows that at the moment t_0 of soliton (8) collission with boundary of sample all spins in the soliton localization region lay in plane Oxz. The magnetization distribution in plane Oxz depends on the sign of h. In negative fields $-\mathrm{ch}^{-1}\rho < h < 0$ the magnetization component $m_1(z, t = t_0)$ steadily increases with movement away from the edge $z = 0$ into the sample. In point $z = 0$ at rather high values $\rho > \mathrm{Arcsh}\,1$ the projection $m_1(z = 0, t = t_0)$ is positive. In this case the component $m_3(z, t = t_0)$ along full length of the sample also behaves also behaves steadily, and magnetization in the soliton at the moment of collision with the boundary turns in plane Oxz by angle lower than 90°

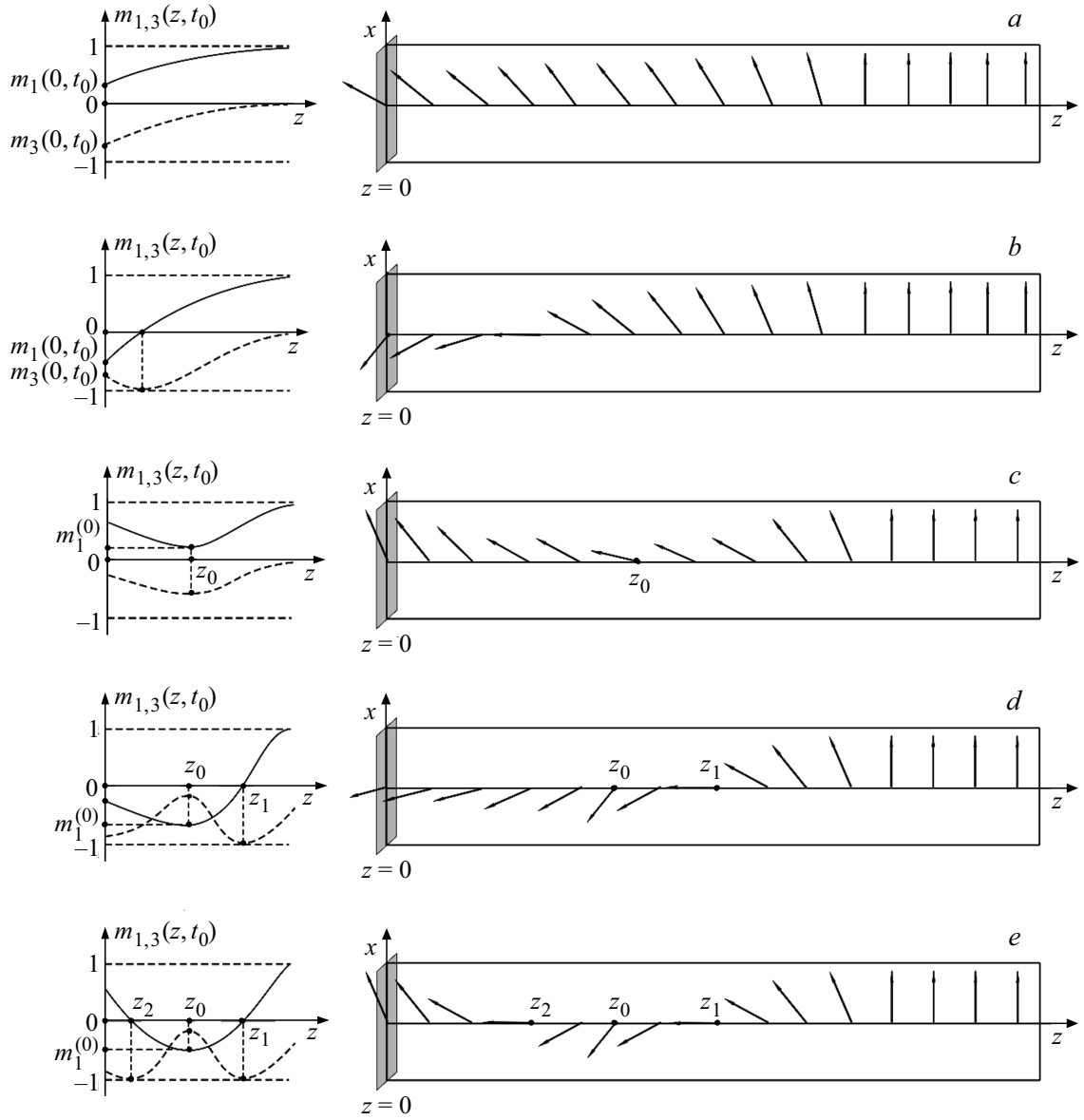

Figure 1. Magnetization components $m_1(z,t_0)$ (solid line), $m_3(z,t_0)$ (dashed line) of soliton (8) and spins distribution at time moment $t=t_0$ at values *a*) $-\mathrm{ch}^{-1}\rho < h < 0$, $\rho >$ Arcsh1; *b*) $-\mathrm{ch}^{-1}\rho < h < 0$, $\rho <$ Arcsh1; *c*) $0 < h < \mathrm{ch}^{-1}\rho$, $\rho >$ Arcsh1; *d*) $0 < h < \mathrm{ch}^{-1}\rho\sqrt{1-\mathrm{sh}^2\rho}$, $\rho <$ Arcsh1; *e*) $\mathrm{ch}^{-1}\rho\sqrt{1-\mathrm{sh}^2\rho} < h < \mathrm{ch}^{-1}\rho$, $\rho <$ Arcsh1. In all cases $c_0 > 0$ was selected.

(see Figure 1, *a*). At relatively low values of $\rho <$ Arcsh1 the projection $m_1(z, t=t_0)$ changes sign from minus to plus when crossing the point determined by the condition $\mathrm{ch}\, y\, \mathrm{sh}\,\rho = 1$, and component $m_3(z, t=t_0)$ at this point has absolute minimum: $m_3 = -1$ (Figure 1, *b*).

In positive fields $0 < h < \mathrm{ch}^{-1}\rho$ near the sample boundary in point $z_0 = \mathrm{ch}\,\rho \ln|f|/2 > 0$ partial remagnetization of medium occurs: $m_1^{(0)} = -1 + 2\,\mathrm{th}^2\rho$. The component $m_1(z, t=t_0)$ has a single minimum at point z_0. As for the component $m_3(z, t=t_0)$, depending on ratio of values of parameter ρ and value of surface field it can have only one ($z=z_0$), two ($z=z_0$ and $z=z_1$), or even three points of extremum ($z=z_0$ and$z=z_{1,2}$). Appropriate cases are shown in Figure 1, *c*–*e*. Additional points $z_{1,2}$ — zero of function $m_1(z, t=t_0)$, determined by equality $\mathrm{ch}[y(z_{1,2})]\,\mathrm{sh}\,\rho = 1$.

At large distances from sample surface at $z \gg 1$ in limit $t \to \pm\infty$ the solution (8) undertakes shape of wave of stationary profile:

$$m_1 = \mathrm{th}\,\xi_\pm,\ m_2 = \mp\mathrm{sign}\,c_0\,\frac{\mathrm{th}\,\rho}{\mathrm{ch}\,\xi_\pm},\ m_3 = -\frac{\mathrm{sign}\,c_0}{\mathrm{ch}\,\rho\,\mathrm{ch}\,\xi_\pm},$$

$$\xi_\pm = (z \mp Vt - z_\pm)/l_0; \quad z_+ = \mathrm{ch}\,\rho \ln(|c_0|/\mathrm{th}\,\rho),$$

$$z_- = -\mathrm{ch}\,\rho \ln(|c_0|\,\mathrm{th}\,\rho/|f|), \qquad (9)$$

which is localized in region with width $l_0 = \mathrm{ch}\,\rho > 1$ and moves with speed $V = \mathrm{th}\,\rho > 0$ inside the sample or towards its surface, parameters $z_\pm$ determine the coordinate

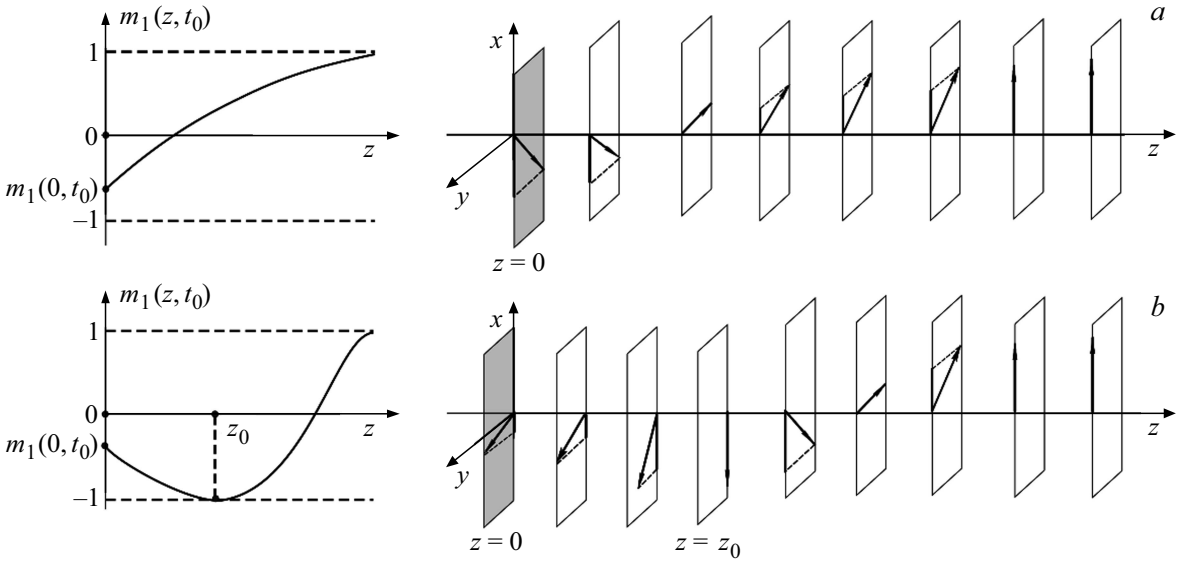

Figure 2. Magnetization component $m_1(z,t_0)$ of soliton (7) and distribution of spins at time moment $t=t_0$ at field values *a*) $h<-\sqrt{2}\,\mathrm{ch}^{-1}\rho$ and *b*) $h>\sqrt{2}\,\mathrm{ch}^{-1}\rho$; in both cases $c_0>0$ was selected.

of the wave center in appropriate reference system, where $z\mp Vt=0$. This is typical soliton of infinite easy-plane ferromagnetic which is called as tuning wave of magnetization [46,26]. The name is associated with that in wave localization region the magnetization turns by 180° from the position $\mathbf{m}=(-1,0,0)$ in soliton tail where $\xi_\pm\ll-1$, to position $\mathbf{m}=(1,0,0)$ in its head, where $\xi_\pm\gg1$. At that in the soliton localization region the projection of vector $\mathbf{m}$ on plane Oyz forms the permanent angle with axis Oz. The magnetization orientation in center of the turning wave after and before reflection is determined by formulas

$$\mathbf{m}=(0,\sin\delta_\pm,\cos\delta_\pm),\ \sin\delta_\pm=\mp\mathrm{sign}\,c_0\,\mathrm{th}\,\rho,$$

$$\cos\delta_\pm=-\mathrm{sign}\,c_0/\,\mathrm{ch}\,\rho.$$

As a result of the turning wave reflection from sample edge its center position shifts by value Δz:

$$\Delta z=z_+-z_-=\mathrm{ch}\,\rho\ln(c_0^2/|f|). \tag{10}$$

From here we find the time of interaction of soliton (8) and sample surface: $|t-t_0|\le\Delta z/V$. Besides, the magnetization in center of soliton (8) after its collision with the boundary turns by angle

$$\delta_+-\delta_-=2\arg[1+i\,\mathrm{sh}\,\rho]=2\,\mathrm{arctg}\,\mathrm{sh}\,\rho. \tag{11}$$

In strong fields at $|h|>\mathrm{ch}^{-1}\rho$ the soliton (7) is described by the expression obtained from (8) using formal replacements:

$$|f|\to f>0,\quad \mathrm{ch}\,y\leftrightarrow\mathrm{sh}\,y,\quad \mathrm{sh}\,s\leftrightarrow\mathrm{ch}\,s.$$

Determinations of y, s stay same. Considering this remark, it is easy to determine that in strong fields the soliton (7) reflection from the sample edge occurs in another plane Oxy. At negative fields $h<-\mathrm{ch}^{-1}\rho$ at moment $t=t_0$ of collision with sample boundary the component m_1 of magnetization while moving into the sample steadily increases. At sample boundary $z=0$ the projection $m_1(z=0,t=t_0)$ is positive at values of field $-\sqrt{2}\,\mathrm{ch}^{-1}\rho<h<-\mathrm{ch}^{-1}\rho$ and negative at $h<-\sqrt{2}\,\mathrm{ch}^{-1}\rho$. The last case is shown in Figure 2, *a*.

At positive values of $h>\mathrm{ch}^{-1}\rho$ in point $z_0=\mathrm{ch}\,\rho(\ln f)/2$, opposite to case of small fields (8), complete remagnetization of medium is observed: $m_1=-1$. The projection m_1 $(z=0,\ t=t_0)$ at the sample boundary is negative at $h>\sqrt{2}\,\mathrm{ch}^{-1}\rho$ (Figure 2, *b*) and positive at $\mathrm{ch}^{-1}\rho<h<\sqrt{2}\,\mathrm{ch}^{-1}\rho$. In Figure 2 in both cases $c_0>0$ is selected. At $c_0<0$ direction of magnetization turning in plane Oxy will be inverse.

At $h>\mathrm{ch}^{-1}\rho$ far away the sample boundary atz $\gg1$, $t\to\pm\infty$ the soliton (7) converts in the turning wave similar to (9):

$$m_1=\mathrm{th}\,\xi_\pm,\quad m_2=-\mathrm{sign}\,c_0\frac{\mathrm{th}\,\rho}{\mathrm{ch}\,\xi_\pm},\quad m_3=\mp\frac{\mathrm{sign}\,c_0}{\mathrm{ch}\,\rho\,\mathrm{ch}\,\xi_\pm},$$

$$\xi_\pm=[z\mp Vt-z_\pm]/l_0,\quad z_+=\mathrm{ch}\,\rho\ln(|c_0|/\,\mathrm{th}\,\rho),$$
$$z_-=-\,\mathrm{ch}\,\rho\ln(|c_0|\,\mathrm{th}\,\rho/f). \tag{12}$$

Comparison of formulas (9) and (12) makes the conclusion that in strong fields h the magnetization in center of soliton (7) after its collision with the ample boundary tuns in plane Oyz by another angle:

$$\delta_+-\delta_-=\pi+2\,\mathrm{arctg}\,\mathrm{sh}\,\rho, \tag{13}$$

which differs from previous angle (11) by π. Shift in soliton position is determined by the previous formula (10).

So, phase change of complex field m_3+im_2 in center of the turning wave after its reflection from the sample

edge in case of weak $|h| < \mathrm{ch}^{-1}\rho$ and strong $|h| > \mathrm{ch}^{-1}\rho$ surface fields is similar to the phase change of light wave during its reflection from the boundary with less and more optically dense medium. In next Section we show that threshold by amplitude of field h nature of change of soliton cores (7) after their reflection from the sample boundary is succeeded by the chiral turning waves in the helicoidal structure. Features of medium remagnetization during chiral waves collision with the sample edge differ from those discussed here in only additional helical rotation of spins in region of soliton cores.

The second class of possible nonlinear excitations in the system if represented by pulsed solitons — breathers [38,39]. In sample thickness the elastically collide with each other and with turning waves of magnetization. The breathers reflection from the sample boundary is also elastic and accompanied by strong deformation of the soliton cores. At far distance from sample surface (at $z \gg 1$, $t \to \pm\infty$) of breather oscillations become regular, it is converted in the precessing breather of the infinite medium [26]:

$$m_1 = 1 - \frac{2}{\tau_\pm}\left[\cos^2 s_\pm + \frac{\cos^2\varphi}{|\sh\mu|^2}\right];$$

$$m_2 = \pm\frac{\mathrm{ctg}\,\varphi}{\tau_\pm|\sh\mu|^2} \times \left[\cos s_\pm \ch y_\pm \sh 2\rho - \sin s_\pm \sh y_\pm \sin(2\varphi)\right],$$

$$m_3 = \frac{2\,\mathrm{ctg}\,\varphi}{\tau_\pm|\sh\mu|^2} \times \left[\sh\rho\cos\varphi\ch y_\pm \sin s_\pm + \ch\rho\sin\varphi\sh y_\pm\cos s_\pm\right], \quad (14)$$

where

$$y_\pm = [z \mp Vt - z_\pm^{(0)}]/l_0, \quad s_\pm = kz \mp \omega t + s_\pm^{(0)},$$

$$\tau_\pm = \cos^2 s_\pm + \mathrm{ctg}^2\varphi\,\mathrm{ch}^2 y_\pm.$$

The soliton (14) is parametrized by complex number $\mu = \rho + i\varphi$; $-\infty < \rho < \infty$, $0 < \varphi < \pi$. Values

$$l_0 = \left(\frac{\ch\rho\sin\varphi}{|\sh\mu|^2}\right)^{-1} > 0, \quad V = \frac{\mathrm{th}\rho(\mathrm{ch}^2\rho + \cos^2\varphi)}{|\sh\mu|^2},$$

$$\omega = \frac{\ch\rho\cos\varphi}{|\sh\mu|^4}(\mathrm{sh}^2\rho - \sin^2\varphi), \quad k = \frac{\sh\rho\cos\varphi}{|\sh\mu|^2}$$

respectively determine the thickness of walls limiting the breather core, movement speed of soliton center, frequency and wave number of oscillations in its core. Within soliton core (14) the magnetization performs inhomogeneous elliptical processing with frequency ω around the axis Ox. The precession ellipse is elongated along the easy-plane Oxy. The precession cone pulses with frequency 2ω. This results in longitudinal oscillations of soliton size. The single result of the breather (14) reflection from the sample boundary is shift of its center

$$z_+^{(0)} = l_0 \ln\left|\frac{\kappa}{\mathrm{th}\rho\,\mathrm{cth}\mu}\right|, \quad z_-^{(0)} = l_0\ln\left|\frac{f}{\kappa\,\mathrm{th}\rho\,\mathrm{cth}\mu}\right|,$$

$$f = \frac{ih\sh\mu + 1}{ih\sh\mu - 1}$$

and change of initial phase of its precession:

$$s_+^{(0)} = \arg\left[\mathrm{th}\rho\,\mathrm{cth}\mu\,\kappa^{-1}\right], \quad s_-^{(0)} = \arg\left[\kappa\,\mathrm{th}\rho\,\mathrm{cth}\mu\,f^{-1}\right].$$

Unlike the case of infinite medium, the breather on half-axis, like the turning wave, can not be fixed ($\rho \neq 0$, $V \neq 0$).

We showed that in limit $|h| \to \infty$ the solution of initial boundary value problem (2), (3) for the semi-infinite sample, comprising N turning waves of magnetization and arbitrary number of breathers and dispersive spin wave packets, transits into the solution of the same model at boundary conditions

$$\mathbf{m}(z=0,t) \to (-1)^N\mathbf{e}_1; \quad \mathbf{m}(z,t) \to \mathbf{e}_1;$$

$$\partial_z\mathbf{m}(z,t) \to 0 \quad \text{at} \quad z \to +\infty.$$

At positive (negative) finite values of the surface field the formation of the half-axis of even (odd) number of turning waves is more energy beneficial. It follows from this that formation of odd or even number of waves in the system can be regulated changing nature of spins securing at the boundary. The determined regularity is kept also for the chiral turning waves.

At weak external effects in sample only dispersive waves without solitons are formed. In case of low amplitude spin waves the magnetization in semi-infinite sample is described by the expressions [38,39]:

$$m_3 = -\frac{2}{\pi}\,\mathrm{Im}\left[\int_0^{+\infty} d\xi\,\frac{b_0(\xi)}{\sh\xi}\,\exp\left(\frac{it\,\ch\xi}{\mathrm{sh}^2\xi}\right) \times \mathrm{Re}\left(\frac{\exp(iz\,\mathrm{sh}^{-1}\xi)}{\mathrm{sh}^{-1}\xi + ih}\right)\right], \; m_1 \approx 1;$$

$$m_2 = \frac{2}{\pi}\,\mathrm{Re}\left[\int_0^{+\infty} d\xi b_0(\xi)\,\mathrm{cth}\,\xi\,\exp\left(\frac{it\,\ch\xi}{\mathrm{sh}^2\xi}\right) \times \mathrm{Re}\left(\frac{\exp(iz\,\mathrm{sh}^{-1}\xi)}{\mathrm{sh}^{-1}\xi + ih}\right)\right]. \quad (15)$$

where b_0 — inverse scattering problem coefficient corresponding to presence of dispersive waves [26].

By direct check we easily make sure that (15) is solution of the linearized Landau–Lifshitz equation (2):

$$\partial_t m_2 + \partial_z^2 m_3 - m_3 = 0, \quad \partial_t m_3 - \partial_z^2 m_2 = 0,$$

$$|m_{2,3}| \ll 1, \quad 0 < z < +\infty$$

With linearized boundary conditions (3), (4):

$$(\partial_z m_{2,3} - h\,m_{2,3})|_{z=0} = 0, \; m_{2,3} \to 0 \quad \text{at} \quad z \to +\infty.$$

3. Solitons of semi-infinite ferromagnetic with helicoidal structure

Let's consider quasi-one-dimensional ferromagnetic crystal without inversion center with energy density:

$$w = \frac{\alpha}{2}(\partial_z \mathbf{M})^2 + \frac{KM_3^2}{2} - \kappa(M_1\partial_z M_2 - M_2\partial_z M_1).$$

Here we use previous marks for medium magnetization $\mathbf{M}(z,t)$ ($\mathbf{M}^2 = M_0^2 = \text{const}$), spatial coordinate $0 < z < \infty$, time t, constants of exchange interaction $\alpha > 0$ and easy-plane anisotropy $K > 0$. Besides, we consider the Dzyaloshinski interaction, to which Lifshitz invariant corresponds

$$-\kappa(M_1\partial_z M_2 - M_2\partial_z M_1),$$

compatible with the uniaxial symmetry of the magnetic crystal without the inversion center. The constant κ can have any sign.

Now, the conditions $\alpha > 0$, $K > 0$ do not ensure stability of the homogeneous state of medium in sample depth (at $z \gg 1$). This turns out to be Inhomogeneous distribution of magnetization of the helicoidal structure type:

$$\mathbf{M} = -M_0(\cos(pz), \sin(pz), 0), \tag{16}$$

where $p = \kappa/\alpha$. Period of magnetic spiral $2\pi/|p|$ is much more the crystallographic periods a: $2\pi\alpha/|\kappa| \gg a$ and usually does not and usually incommensurate with them.

Let, as previously, along the boundary $z = 0$ of sample we apply the effective field of unidirectional surface anisotropy $\mathbf{H} = H\mathbf{e}_1$, where $\mathbf{e}_1 = (1, 0, 0)$. In sample thickness the helical ordering corresponds to energy density $-M_0^2\kappa^2/(2\alpha)$. We will take the system energy from the helicoidal ground state of the medium at $z \gg 1$. Then total energy of sample will be written as follows

$$E = \frac{1}{2}\int_0^\infty \mathrm{d}z \left[\alpha(\partial_z \mathbf{M})^2 + KM_3^2 + \frac{M_0\kappa^2}{\alpha} - 2\kappa(M_1\partial_z M_2 - M_2\partial_z M_1)\right] + HM_1|_{z=0}. \tag{17}$$

Let's go to dimensionless variables:

$$\mathbf{m} = -\mathbf{M}/M_0, \quad \tilde{z} = z\left[\frac{1}{\alpha}\left(K + \frac{\kappa^2}{\alpha}\right)\right]^{1/2},$$

$$\tilde{t} = \gamma M_0 t\left(K + \frac{\kappa^2}{\alpha}\right), \quad \tilde{h} = \frac{H}{M_0}\left[\alpha\left(K + \frac{\kappa^2}{\alpha}\right)\right]^{-1/2},$$

which coincide with previous (1) at $\kappa = 0$. In new variables the system energy looks like

$$\tilde{E} = \frac{E}{M_0^2}\left[\alpha\left(K + \frac{\kappa^2}{\alpha}\right)\right]^{-1/2} = \frac{1}{2}\int_0^\infty \mathrm{d}\tilde{z}[(\partial_{\tilde{z}}\mathbf{m})^2 + (1-q^2)m_3^2 - 2q(m_1\partial_{\tilde{z}}m_2 - m_2\partial_{\tilde{z}}m_1) + q^2] - \tilde{h}\,m_1|_{\tilde{z}=0}.$$

Helical structure (16) corresponds field distribution $\mathbf{m}$:

$$\mathbf{m} = (\cos(q\tilde{z}), \sin(q\tilde{z}), 0), \tag{18}$$

where $q = \kappa/[\alpha(K + \kappa^2/\alpha)]$.

Possible nonlinear excitations of the helicoidal structure of semi-infinite ferromagnetic sample correspond to solutions of Landau–Lifshitz equation:

$$\partial_{\tilde{t}}\mathbf{m} = [\mathbf{m} \times \partial_{\tilde{z}}^2\mathbf{m}] - (1-q^2)(\mathbf{e}_3 \cdot \mathbf{m})[\mathbf{m} \times \mathbf{e}_3] + 2q(\mathbf{e}_3 \cdot \mathbf{m})\partial_{\tilde{z}}\mathbf{m}, \tag{19}$$

where $\mathbf{m}^2 = 1$, $0 < \tilde{z} < \infty$, with boundary conditions:

$$[\mathbf{m} \times (\partial_{\tilde{z}}\mathbf{m} + q[\mathbf{m} \times \mathbf{e}_3] + \tilde{h}\,\mathbf{e}_1)]|_{\tilde{z}=0} = 0,$$

$$\mathbf{m} \to (\cos(q\tilde{z}), \sin(q\tilde{z}), 0) \quad \text{at} \quad \tilde{z} \to +\infty \tag{20}$$

and specified initial perturbation of the helical structure:

$$\mathbf{m}(\tilde{z}, \tilde{t} = 0) = \mathbf{m}_0(\tilde{z}), \tag{21}$$

Which is compatible with conditions (20). Vector $\mathbf{e}_3 = (0, 0, 1)$, like previously, specifies direction of the „hard-axis" of magnetization.

To determine relationship between the problems (2)–(5) and (19)–(21) we will use parameterization of the normalized magnetization by angles Θ and Φ:

$$\mathbf{m} = (\cos\Theta\cos\Phi, \cos\Theta\sin\Phi, \sin\Theta).$$

Landau–Lifshitz equation (19) together with the boundary conditions (20) follows from Hamilton variation principle for action functional:

$$S = \int_0^\infty \mathrm{d}\tilde{z}\left(\sin\Theta\,\partial_{\tilde{t}}\Phi - \frac{1}{2}[(\partial_{\tilde{z}}\Theta)^2 + \cos^2\Theta(\partial_{\tilde{z}}\Phi - q)^2 + \sin^2\Theta]\right) + \tilde{h}\cos\Theta\cos\Phi|_{z=0}. \tag{22}$$

The initial boundary value problem (2)–(5) for the easy-plane ferromagnetic with homogeneous ground state is described by action that follows from (22) at $q = 0$. From here the important statement follows, it is summary of determined in [26,29] for infinite medium. If we know solution $\Theta^{(l)}(z,t,h)$, $\Phi^{(l)}(z,t,h)$ of Landau–Lifshitz equation (2) with boundary conditions (3) and (4), then the solution $\Theta^{(g)}(\tilde{z},\tilde{t},\tilde{h},q)$, $\Phi^{(g)}(\tilde{z},\tilde{t},\tilde{h},q)$ of model (19), (20) of chiral ferromagnetic is determined by formulas

$$\Phi^{(g)}(\tilde{z},\tilde{t},\tilde{h},q) = \Phi^{(l)}(z = \tilde{z}, t = \tilde{t}, h = \tilde{h}) + q\tilde{z},$$

$$\Theta^{(g)}(\tilde{z},\tilde{t},\tilde{h},q) = \Theta^{(l)}(z = \tilde{z}, t = \tilde{t}, h = \tilde{h}).$$

After shown transformation the action functional of one problem transits into the functional of another problem. This justifies equivalence of not only equations, but also of initial boundary value conditions for two problems. Distribution

of magnetization $\mathbf{m}^{(l)}(z,t,h)$ and $\mathbf{m}^{(g)}(\tilde{z},\tilde{t},\tilde{h},q)$ of these problems are related to each other:

$$m_+^{(g)}(\tilde{z},\tilde{t},\tilde{h},q) = m_+^{(l)}(z=\tilde{z},t=\tilde{t},h=\tilde{h})\,\mathrm{e}^{iq\tilde{z}},$$

$$m_3^{(g)}(\tilde{z},\tilde{t},\tilde{h},q) = m_3^{(l)}(z=\tilde{z},t=\tilde{t},h=\tilde{h}), \qquad (23)$$

where $m_+ = m_1 + im_2$. When comparing solutions (23) the interaction constants also change.

In particular, low-amplitude spin wave field in semi-infinite sample of the chiral ferromagnetic looks like

$$\mathbf{m}^{(g)} = \mathbf{n} + \left(m_2^{(l)}[\mathbf{e}_3\times\mathbf{n}] + m_3^{(l)}\mathbf{e}_3\right)\big|_{z=\tilde{z},t=\tilde{t},h=\tilde{h}},$$

$$\mathbf{n} = (\cos(q\tilde{z}),\sin(q\tilde{z}),0), \qquad (24)$$

where functions $m_{2,3}^{(l)}$ are determined by formulas (23). By direct check we can easily make sure that expression (24) satisfies the linearized Landau–Lifshitz equation (19) with linearized boundary condition (20).

The turning wave (7) of the ferromagnetic with homogeneous ground state after conversion (23) converts into the chiral turning wave in semi-infinite ferromagnetic with helicoidal structure:

$$m_1^{(g)} = m_1^{(l)}\cos(q\tilde{z}) - m_2^{(l)}\sin(q\tilde{z}),$$

$$m_2^{(g)} = m_1^{(l)}\sin(q\tilde{z}) + m_2^{(l)}\cos(q\tilde{z}),\ m_3^{(g)} = m_3^{(l)}, \qquad (25)$$

where expressions $m_j^{(l)}$ are determined by formulas (7) considering replacement $z\to\tilde{z},\ t\to\tilde{t},\ h\to\tilde{h}$. At large distances from the sample edge the solution (25) describes the simplest soliton of infinite medium [26,29]. The magnetization in such soliton can be turned either against diretion of turning of magnetic spiral (18), which, respectively, results in decrease or increase of the spiral pitch. Both are accompanied by exit of the magnetic moments from plane Oxy.

Near the sample surface the core of the chiral soliton (25) strongly deforms, after this it elastically reflects from the sample boundary and restores its stationary shape. As result of reflection the center of chiral wave shifts by value Δz (10).

The chiral solitons succeed basic dynamic properties of solitons of Section 2.

Let's specify the made general remarks. Let's consider that the parameter $\rho > 0$. To simplify the analysis we assume that presence of soliton does not change direction of turning of spiral (18), and results only in decrease or increase of its pitch. Then in case of weak surface anisotropy $|h| < \mathrm{ch}^{-1}\rho$ at value of integration constant $c_0 > 0$ ($c_0 < 0$) before collision with the sample boundary in the localization region of soliton (25) the spiral pitch decreases (increases), and after collision — increases (decreases). At that along full length of sample at $c_0 > 0$ the spins are inclined towards the boundary, and at $c_0 < 0$ — from boundary. During soliton reflection in from the sample edge in its center the projection of magnetization $m_3^{(g)}$ on the spiral axis does not change (see formulas (9) and (25)). At moment $t = t_0$ (see (8)) of soliton (25) collision with the sample boundary the spiral pitch and phase of spins turning within soliton exactly coincide with same on the helical structure (18), and soliton presence in the structure can be observed only by spins exit from the turning plane Oxy.

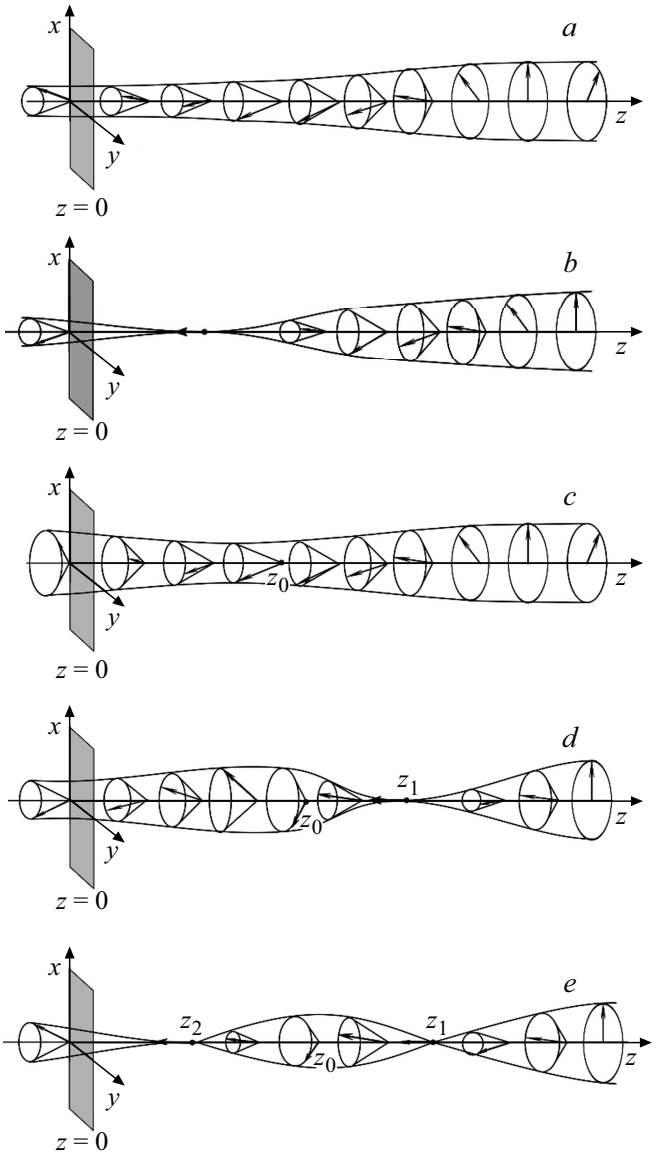

Figure 3. Spins location in soliton (25) at moment $t = t_0$ of collision with sample boundary at values *a*) $-\mathrm{ch}^{-1}\rho < h < 0$, $\rho > \mathrm{Arcsh1}$; *b*) $-\mathrm{ch}^{-1}\rho < h < 0$, $\rho < \mathrm{Arcsh1}$; *c*) $0 < h < \mathrm{ch}^{-1}\rho$, $\rho > \mathrm{Arcsh1}$; *d*) $0 < h < \mathrm{ch}^{-1}\rho\sqrt{1-\mathrm{sh}^2\rho}$, $\rho < \mathrm{Arcsh1}$; *e*) $\mathrm{ch}^{-1}\rho\sqrt{1-\mathrm{sh}^2\rho} < h < \mathrm{ch}^{-1}\rho$, $\rho < \mathrm{Arcsh1}$. In all cases $c_0 > 0$ was selected.

In weak negative fields $-\mathrm{ch}^{-1}\rho < h < 0$ at rather high large values of $\rho > \mathrm{Arcsh1}$ the magnetization component $m_3(z,t_0)$ is monotonous while moving into the sample. This means that in this case the envelope of the soliton at $t = t_0$ is most narrow in point $z = 0$ at its boundary (Figure 3, *a*). At relatively small $\rho < \mathrm{Arcsh1}$ the projection

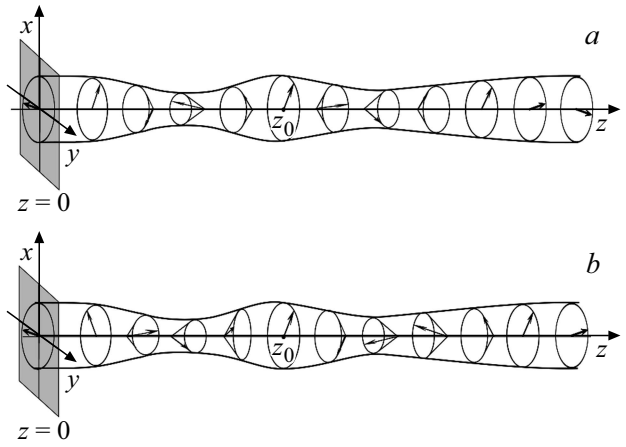

Figure 4. Spins location in soliton (25) in case of large positive fields $h > \mathrm{ch}^{-1}\rho$ directly *a*) before and *b*) after collision with sample boundary; $c_0 > 0$ was selected. At the moment of collision the spins along the entire sample lay in plane Oxy.

$m_3^{(g)}$ reaches absolute minimum -1 in point determined by the condition $\mathrm{ch}\, y\, \mathrm{sh}\rho = 1$ (Figure 3, *b*). In positive fields $0 < h < \mathrm{ch}^{-1}\rho$ at rather large values $\rho > \mathrm{Arcsh1}$ the magnetization component $m_3^{(g)}(z, t_0)$ has only one point of extremum $z_0 = \mathrm{ch}\rho \ln|f|/2 > 0$ near the boundary (Figure 3, *c*). The soliton envelope is compressed in point $z = z_0$, and extends at both sides of the point z_0, gradually reaching the limit value corresponding to the helicoidal structure (18). At relatively small $\rho < \mathrm{Arcsh1}$ depending on values of field h the component $m_3^{(g)}(z, t_0)$ obtains one more or two additional points of absolute minimum $z_{1,2}$, determined by the condition $\mathrm{ch}[y(z_{1,2})]\, \mathrm{sh}\rho = 1$ (Figure 3, *d* and *e*). In these points the magnetization is parallel to the „hard-axis“ of bulk anisotropy: $\mathbf{m}^{(g)} = (0, 0, -1)$.

Cases in Figure 3, *a*–*e* are similar to those in Figure 1, *a*–*e*. Ranges of values of the surface field, given in text to Figure 3, *a*–*e*, exactly coincide with the same in Figure 1, *a*–*e*.

At strong surface anisotropy $|h| > \mathrm{ch}^{-1}\rho$ the component $m_3^{(g)}$ in center of soliton after reflection changes the sign (see (12), (25)). This means that as results of interaction of soliton (25) with the sample boundary in inclination of spins towards the boundary or from the boundary changes to opposite (Figure 4, *a* and *b*). Just at the moment $t = t_0$ of soliton collision with the sample surface the magnetization component $m_3^{(g)} = 0$, and, hence, spins in the entire sample lie in plane Oxy. In soliton, built in the helical structure, the spins inclination (towards the sample boundary or from it) depends on sign of parameters h and c_0 like in „seed“ soliton in ferromagnetic with homogeneous ground state.

Note that unlike the case of small fields $|h| < \mathrm{ch}^{-1}\rho$, in strong filds $|h| > \mathrm{ch}^{-1}\rho$ the direction of turning of soliton (25) during reflection from the sample boundary does not change. In localization region of soliton the spiral pitch (18) at $c_0 > 0$ ($c_0 < 0$) both before, and after soliton collision with the sample boundary is increased (decreased) as compared to pitch of the helical structure (compare formulas (12), (18)).

As a conclusion let's discuss the chiral breather. The breather solution of the easy-plane ferromagnetic [38,39] under action of conversion (25) transits into pulsed soliton on the background of helical structure (18). Figure 5, *a* and *b* schematically shows such soliton far from sample edge (at $z \gg 1$) at time moments $t = 0$ and $t = T/2$, where $T = 2\pi/\omega$ — period of pulsations. In center of soliton — point z_0 — the magnetization component $m_3^{(g)}$ reaches the extreme value, and the vector $\mathbf{m}^{(g)}(z, t)$ periodically changes inclination from the direction towards the sample boundary to the direction into the sample. In the soliton the stretching regions of the helical structure alternate with compression regions. In Figure 5, *a* at $t = 0$ to the right of the center of soliton (in region $z > z_0$) the helical structure is stretched, and to the left of the center (in region $z < z_0$) — it is compressed. After half-period of oscillations, at $t = T/2$ (Figure 5, *b*) the spiral stretching at right of the center of soliton changes by its compression, and compression of spiral to the left of the center of soliton changes by stretching. At that the projection $m_3^{(g)}$ both to the right, and to the left of the center periodically changes the sign to opposite.

Besides, heterogeneity of the precession of magnetization and pulsations in the breather core result in small longitudinal oscillations of soliton along the axis of magnetic spiral. They are not shown in Figure 5.

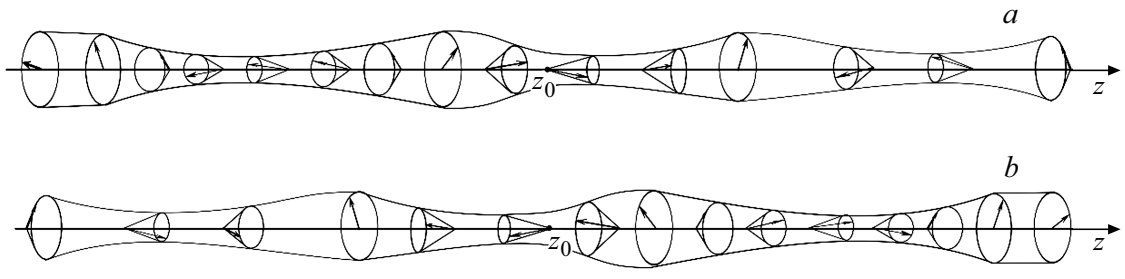

Figure 5. Spins location in pulsed soliton — breather — on background of helical structure (18) far from sample boundary at time moments *a*) $t = 0$ and *b*) $t = T/2$, where$T$ — period of pulsations.

4. Conclusion

Method of inverse scattering problem in combination with the special conversion of solutions of model of semi-infinite ferromagnetic with the ground state used to prepare and to analyze the new class of explicit solutions of Landau–Lifshitz equation describing distribution spreading of dispersive waves and solitons along the helicoidal structure of the semi-infinite inverse scattering ferromagnetic with anisotropy of „easy-plane“ type. At sample boundary the boundary condition was considered, it corresponds to partial securing of the helicoidal structure. Its boundary cases correspond to free edge spins and complete securing of magnetization at the sample boundary. Soliton-like nuclei of the helicoidal phase on the background of homogeneous distribution of magnetization in the semi-infinite ferromagentic with anisotropy of „easy axis“ type can also be studied using the suggested approach. For this it is sufficient to use formulas in paper [37] for solitons in semi-infinite easy-axis ferromagnetic with homogeneous ground state.

If Dzyaloshinski interaction is absent the easy-plane ferromagnetic has two classes of solitons. One of them comprises turning waves of magnetization, which remind the moving 180- domain walls. Second type of solitons — pulsed solitons with magnetization precession near the „easy-plain“. Dzyaloshinski interaction determines the formation of the helicoidal structure and built-in solitons. It is important that chiral solitons are inseparable from the helical structure. They succeed some features of solitons of the ferromagnetic with homogeneous ground state and obtain new features. If the turning waves with different turning of magnetization on the background of homogeneous state of medium have same energy, then corresponding to them chiral turning waves significantly differ in core structure, and hence, in energy. The energy of the magnetic soliton in the helicoidal structure shall mean the difference between the energy of system with soliton in it and energy of helicoidal ground state of medium without soliton. The correct calculation of such energy — is theme of separate study. Dependence of energy of chiral solitons on the parameters of the helicoidal structure and surface anisotropy shall be considered, for example, when describing the thermodynamic properties of solitons system in semi-infinite sample.

It is determined that structure of chiral turning waves (7), (25) after reflection from the sample surface depends in threshold manner on the amplitude of the surface field h. Besides, „deformation“ of soliton core at the time of the collision with the sample surface significantly depends on sign of h. The chiral breathers, unlike the chiral turning waves, have characteristic frequencies of internal pulsations. So, the breathers can be detected by the resonance absorption of energy at frequencies of their oscillations.

All types of solitons in the helicoidal structure are movable particle-like objects. The experimental confirmation of regularities of their elastic reflection from sample boundaries determined during study is actual.

Collision of chiral solitons with sample surface is accompanied by significant change in their internal structure and dynamic properties, and also by processes of medium remagnetization by value equal to about saturation magnetization. So, the chiral solitons in semi-infinite sample can not be described by the traditional method of perturbation theory for infinite medium. This supposes sufficient „hardness“ of soliton cores and small changes of their properties under effect of perturbations.

The study results shall be considered during modeling of soliton processes near surface of actual ferromagnetics with helicoidal structure. The obtained analytical solutions are useful for numerical calculations verification.

Funding

This study was carried out as part of project of RSF No. 19-72-30028.

Conflict of interest

The authors declare that they have no conflict of interest.

References

[1] L.D. Landau, E.M. Lifshitz. Elektrodinamika sploshnykh sred (seriya „Teoreticheskaya fizika“, t. VIII). Nauka, M. (1982) 620 s. (in Russian).
[2] I.E. Dzyaloshinskii. Sov. Phys. JETP **20**, *3*, 665 (1965).
[3] T. Moriya. Phys. Rev. **120**, *1*, 91 (1960).
[4] Yu.A. Izyumov. Sov. Phys. Usp. **27**, *9*, 845 (1984).
[5] Yu.A. Izyumov. Difraktsiaya neitronov na dlinnoperiodicheskih strukturah. Energoatomizdat, M. (1987). S. 180–181.
[6] V.D. Buchel'nikov, I.V. Bychkov, V.G. Shavrov. J. Magn. Magn. Mater. **118**, *1–2*, 169 (1993).
[7] A.A. Fraerman, O.G. Udalov. Phys. Rev. B **77**, *9*, 094401 (2008).
[8] I.V. Bychkov, D.A. Kuzmin, V.G. Shavrov. J. Magn. Magn. Mater. **329**, 142 (2013).
[9] A.A. Tereshchenko, A.S. Ovchinnikov, I. Proskurin, E.V. Sinitsyn, J. Kishine. Phys. Rev. B **97**, *18*, 184303 (2020).
[10] J. Kishine, A.S. Ovchinnikov. Phys. Rev. B **101**, *18*, 184425 (2020).
[11] Yu.B. Kudasov. Phys. Solid State **65**, *6*, 898 (2023).
[12] J. Kishine, A.S. Ovchinnikov. Solid State Phys. **66**, 1 (2015).
[13] J. Kishine, A.S. Ovchinnikov, I.V. Proskurin. Phys. Rev. B **82**, 064407 (2010).
[14] K. Tokushuku, J. Kishine, M. Ogata. J. Phys. Soc. Jpn. **86**, *12*, 124701 (2017).
[15] V. Laliena, S. Bustingorry, J. Campo. Sci. Rep. **10**, *1*, 20430 (2020).
[16] S.A. Osorio, A. Athanasopoulos, V. Laliena, J. Campo, S. Bustingorry. Phys. Rev. B **106**, *9*, 094412 (2022).
[17] K. Adachi, N. Achiwa, M. Mekata. J. Phys. Soc. Jpn. **49**, *2*, 545 (1980).
[18] A. Zheludev, S. Maslov, G. Shirane, Y. Sasago, N. Koide, K. Uchinokura. Phys. Rev. Lett. **78**, *25*, 4857 (1997).
[19] B. Roessli, J. Schefer, G.A. Petrakovskii, B. Ouladdiaf, M. Boehm, U. Staub, A. Vorotinov, L. Bezmaternikh. Phys. Rev. Lett. **86**, *9*, 1885 (2001).

[20] S. Ohara, S. Fukuta, K. Ohta, H. Kono, T. Yamashita, Y. Matsumoto, J. Yamaura. JPS Conf. Proc. **3**, 017016 (2014).
[21] Y. Kousaka, T. Ogura, J. Zhang, P. Miao, S. Lee, S. Torii, T. Kamiyama, J. Campo, K. Inoue, J. Akimitsu. J. Phys.: Conf. Ser. **746**, *1*, 012061 (2016).
[22] T. Matsumura, Y. Kita, K. Kubo, Y. Yoshikawa, S. Michimura, T. Inami, Y. Kousaka, K. Inoue, S. Ohara. J. Phys. Soc. Jpn. **86**, *12*, 124702 (2017).
[23] Y. Togawa, T. Koyama, K. Takayanagi, S. Mori, Y. Kousaka, J. Akimitsu, S. Nishihara, K. Inoue, A.S. Ovchinnikov, J. Kishine. Phys. Rev. Lett. **108**, *10*, 107202 (2012).
[24] A.B. Borisov, V.V. Kiselev. Dvumernye i trekhmernye magnitnye topologicheskie defekty, solitony i tekstury v magnetikakh. Fizmatlit, M. (2022), 456 s. (in Russian).
[25] A.B. Borisov, J. Kishine, I.G. Bostrem, A.S. Ovchinnikov. Phys. Rev. B **79**, *13*, 134436 (2009).
[26] A.B. Borisov, V.V. Kiselev. Kvaziodnomernye magnitnye solitony. Fizmatlit, M. (2014). 520 s. (in Russian).
[27] V.V. Kiselev, A.A. Raskovalov. JETP **116**, *2*, 272 (2013).
[28] V.V. Kiselev, A.A. Raskovalov. Chaos, Solitons & Fractals **84**, 88 (2016).
[29] A.B. Borisov, Yu.A. Izyumov. Dokl. AN SSSR **283**, *4*, 859 (1985). (in Russian).
[30] T.H. Kim, S.H. Han, B.K. Cho. Commun. Phys. **2**, *1*, 41 (2019).
[31] I.T. Khabibullin. Theor. Math. Phys. **86**, *1*, 28 (1991).
[32] A.S. Fokas. Commun. Math. Phys. **230**, *1*, 1 (2002).
[33] E.K. Sklyanin. Func. Anal. Its. Appl. **21**, *2*, 164 (1987).
[34] P.N. Bibikov, V.O. Tarasov. Theor. Math. Phys. **79**, *3*, 570 (1989).
[35] A.S. Fokas. Physica D **35**, *1–2*, 167 (1989).
[36] V.V. Kiselev. JETP **136**, *3*, 330 (2023).
[37] V.V. Kiselev. Theor. Math. Phys. **219**, *1*, 576 (2024).
[38] V.V. Kiselev, A.A. Raskovalov. Bulletin of RUS **88**, *9*, 1382 (2024).
[39] V.V. Kiselev, A.A. Raskovalov. Chaos, Solitons & Fractals **188**, 115500 (2024).
[40] W.H. Meiklejohn, C.P. Bean. Phys. Rev. **102**, *5*, 1413 (1956).
[41] W.H. Meiklejohn, C.P. Bean. Phys. Rev. **105**, *3*, 904 (1957).
[42] B.N. Filippov. Mikromagnitnye struktury iikh nelinejnye svojstva, Chast 1. UrO RAN, Ekaterinburg (2019). 423 s. (in Russian).
[43] J. Nogués, I.K. Schuller. J. Magn. Magn. Mater. **192**, *2*, 203 (1999).
[44] E.M. Lifshitz, L.P. Pitaevsky. Statisticheskaya fizika, ch. 2. Teoriya kondensirovannogo sostoyaniya (seriya „Teoreticheskaya fizika“, t. IX). Nauka, M. (1978). 448 s. (in Russian).
[45] A.I. Akhiezer, V.G. Baryakhtar, S.V. Peletminskiy. Spinovye volny. Nauka, M. (1967). 368 s. (in Russian).
[46] I.A. Akhiezer, A.E. Borovik. JETP **25**, *5*, 885 (1967).

Translated by I.Mazurov